Annals of Nuclear Medicine
https://doi.org/10.1007/s12149-019-01399-w

ORIGINAL ARTICLE

Computer-aided detection of bone metastasis in bone scintigraphy images using parallelepiped classification method

Florina-Gianina Elfarra[1,2] · Mihaela Antonina Calin[3] · Sorin Viorel Parasca[4]

Received: 18 July 2019 / Accepted: 26 August 2019

Abstract

Objective Accurate diagnosis of metastatic tissue on bone scintigraphy images is of paramount importance in making treatment decisions. Although several automated systems have developed, more and better interpretation methods are still being sought. In the present study, a new modality for bone metastasis detection from bone scintigraphy images using parallelepiped classification (PC) as method for mapping the radionuclide distribution is presented.

Methods Bone scintigraphy images from 12 patients with bone metastases were analyzed using the parallelepiped classifier that generated color maps of scintigraphic images. Seven classes of radionuclide accumulation have been identified and fed into machine learning software. The accuracy of the proposed method was evaluated by statistical measurements in a confusion matrix. Overall accuracy, producer's and user's accuracies and κ coefficient were computed from each confusion matrix associated with the individual case.

Results The results revealed that the method is sufficiently precise to differentiate the metastatic bone from normal tissue (overall classification accuracy $= 87.58 \pm 2.25\%$ and κ coefficient $= 0.8367 \pm 0.0252$). The maps are easier to read (due to better contrast) and can detect even slightest differences in accumulation levels among pixels.

Conclusions In conclusion, these preliminary data suggest that bone scintigraphy combined with PC method could play an important role in the detection of bone metastasis, allowing for an easier but correct interpretation of the images, with effects on the diagnosis accuracy and decision making on the treatment to be applied.

Keywords Cancer · Bone · Nuclear imaging · Radionuclide accumulation · Parallelepiped classification · Machine learning

Introduction

Bone metastasis is a frequent cancer complication that occurs due to the spread of cells from certain types of primary tumors, especially that arising in the breast, prostate and lung [1] to the bone. Early diagnosis of bone metastases has a major impact on treatment decision and at the same time it is a decisive factor in the evolution of the disease and the quality of life. Diagnosis of bone metastases is usually based on the combined analysis of signs and symptoms (bone pain, fractures, nerve problems, loss of appetite, fatigue, confusion, hypercalcemia, etc.) with imaging data [2]. Different imaging methods are now used in clinical practice for the diagnosis of bone metastases such as X-rays, computed tomography, magnetic resonance imaging, and positron emission tomography, but bone scintigraphy is considered the golden standard [3–5].

Interpretation of bone scintigraphy is done by physicians, most often by visual examination, which makes the

✉ Mihaela Antonina Calin
mantonina_calin@yahoo.com; micalin@inoe.ro

Florina-Gianina Elfarra
gianina.elfarra@gmail.com

Sorin Viorel Parasca
sorinparasca@yahoo.com

1 "Saint John" Emergency Clinical Hospital, 13 Vitan-Barzesti Street, Bucharest, Romania

2 Faculty of Physics, The University of Bucharest, 405 Atomistilor Street, 077125 Magurele, Romania

3 National Institute of Research and Development for Optoelectronics INOE 2000, 409 Atomistilor Street, P.O. Box MG5, 077125 Magurele, Ilfov, Romania

4 Carol Davila University of Medicine and Pharmacy, 37 Dionisie Lupu Street, 020022 Bucharest, Romania

Published online: 06 September 2019

results largely dependent on the experience and personality of the observers with effects on the diagnosis accuracy and decision making on the treatment to be applied. One way to avoid human subjectivism could be to use a computer system to classify scintigraphy data according to user-defined criteria and to propose a version for image interpretation. The development of computer-aided diagnosis (CAD) systems began in the 1960s [6]. Since then, many CAD systems have been developed, which are currently used in medical imaging field, particularly in radiography, computed tomography, nuclear magnetic resonance and ultrasound, for the diagnosis of breast cancer [7], lung cancer [8], colon cancer [9], prostate cancer [10], coronary artery disease [11], Alzheimer's disease [12], etc. CAD systems have also been developed for bone scintigraphy. Thus, Erdi et al. [13] proposed a semi-automatic image segmentation method that allows quantification of bone metastases from whole body scintigraphy. A characteristic-point-based fuzzy inference system (CPFIS) was also developed by Yin and Chiu [14]. The CPFIS system allows the localization of bone lesions in the human body using asymmetry and brightness as features for classification of scintigraphy data. Fully automated CAD systems for bone scintigraphy have also been developed since 2005, when Sajn et al. [15] proposed the first machine learning-based expert system for automated diagnostics. Some of them are already integrated into software packages that are now commercially available, such as Exini bone and Bonenavi. Exini bone (EXINI Diagnostics AB, Lund, Sweden) is a fully automated CAD system based on image-processing techniques and artificial neural networks (ANN) originally developed in 2008 [16] to interpret bone scans and determine the presence or absence of bone metastases. Bonenavi (Fujifilm RI Pharma, Tokyo, Japan) is also a fully automated CAD system that uses artificial neural networks and Japanese databases for identification of bone metastasis [5, 17, 18]. These software systems have exhibited good diagnostic accuracy and reproducibility [5], but their strong dependence on training databases may affect data classification results [18]. Future studies are aimed at improving the performance of these software [19]. Nowadays, the development of new automated CAD systems and the continuous improvement of the performance of existing CAD systems in the interpretation of bone scintigraphy images are current research topics in scintigraphy field.

This paper proposes a new modality for bone metastasis detection from bone scintigraphy images using parallelepiped classification (PC) as method for mapping the radionuclide distribution. We considered that this method could be one suitable for an easy interpretation of bone scintigraphy images being one of the simplest and fastest classification methods with reasonable performance and low computational time.

The main objectives were: (1) identification of appropriate methods for bone scintigraphy image processing; (2) generation of radionuclide distribution map and detection of bone metastasis; (3) assessment of method performances and (4) establishing future research directions to extend the applicability of the method to other types of scintigraphy.

Materials and methods

Bone scintigraphy

Twelve patients aged between 41 and 77 years (mean age ± standard deviation: 61.08 ± 12.48 years) with suspected bone metastases were selected for this preliminary study. Bone scintigraphy was performed 2 h after intravenous injection of 629 MBq (17mCi) of ^{99m}Tc-hydroxydiphosphonate (^{99m}Tc-HDP) (Mallinckrodt Medical B.V., Petten, The Netherlands) using a gamma-camera system (Symbia T2, Siemens Medical Systems Inc. USA) equipped with a low energy high resolution (LEHR) collimator. Whole-body anterior and posterior images were acquired at a scan speed of 12 cm/min, 256 × 1024 matrix and zoom factor of 1. The energy window was set at ± 15% of the energy peak of ^{99m}Tc (140 keV). The images were initially saved in DICOM format which can be read by any computer, making possible further processing and analysis. The procedures performed in this study involving human participants were in accordance with the ethical standards of the "Saint John" Emergency Clinical Hospital Research Committee and with the 1964 Helsinki declaration and its later amendments or comparable ethical standards.

Parallelepiped classifier-based methodology for the detection of bone metastases in bone scintigraphy images (PC-BS)

The PC-BS method proposed in this study consists of three main steps: (1) bone scintigraphy image processing; (2) bone scintigraphy image analysis and (3) evaluation of results (Fig. 1).

Bone scintigraphy image processing

Bone scintigraphy images are often distorted by noise interfering with the signal of the gamma-camera system which leads to false information during analysis and affects diagnostic accuracy. Therefore, noise reduction in bone scintigraphy images is an indispensable process for producing accurate results. Over the years, various methods to remove noise from a scintigraphy image have been proposed, such as linear filters, median filter, Butterworth filter, and Wiener filter. However, it has been shown that these filters sometimes

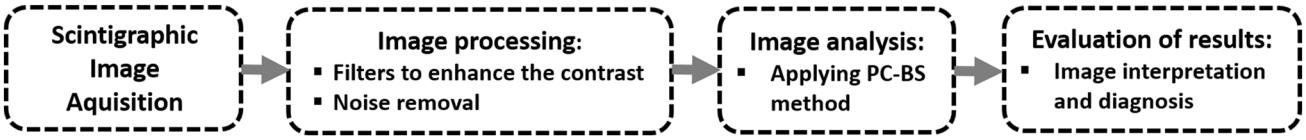

Fig. 1 Flowchart illustrating the steps of the proposed PC-BS methodology

reduce the edge information in the denoising process [20]. In this study, an adaptive filtering technique based on the Kuwahara filter [21] was used to suppress the noise. This filter is able to apply the smoothing on the image while preserving the position and magnitude of edges. The Kuwahara filter works by selecting a kernel window of size ($n \times n$; n being an odd number) around each pixel $p(x, y)$ in a gray-level image. The kernel window of the filter is then divided into four overlapping square sub-windows having the pixel $p(x, y)$ as a corner. The mean value and variance of each sub-window are calculated and the initial value of the pixel $p(x, y)$ is replaced by the mean value of the sub-window with the smallest variance. In this study, the Kuwahara filter with the 3×3 kernel window was used to let only relatively homogeneous data contribute to the output image.

Bone scintigraphy image analysis

The overall goal of the image analysis stage is to automatically categorize all pixels in a bone scintigraphy image in individual classes based on the pixel values generating bone classification map. The PC method, with origins in the remote sensing domain, was chosen in this study to achieve this objective. The PC method, also called the level-slice classifier (LSC) [22], is a supervised method that performs pixel classification of an input image using a simple decision rule that involves finding the minimum and maximum pixels values for each class. This is usually done in terms of the mean values of each class plus and minus a given number of standard deviations. The extreme values of each class form rectangular or parallelepiped boxes as decision boundaries for assigning the pixels. Pixels will be tested against each parallelepiped box to determine their membership. An unknown pixel will be assigned to a particular class if its value lie inside the parallelepiped decision boundaries of that class. If the pixel value lies outside the parallelepiped decision boundaries for all classes, it will be assigned to an unclassified category.

In this study, for proper mapping of bone tissues characteristics using the PC method, a reference dataset representative for seven classes of bone tissues identified in the skeletal area (normal bone tissue with low density, normal bone tissue with intermediate low density, normal bone tissue with intermediate high density, normal bone tissue with high density, perimetastatic bone tissue with significant radionuclide accumulation, metastatic bone tissue with high radionuclide accumulation, metastatic bone tissue with very high radionuclide accumulation) was selected, directly from the original bone scintigraphy image, based on the visual examination of the image by a clinician. For each of the selected bone classes, the mean value and standard deviation were calculated to define the decision boundaries of the PC. After several tests, the performance of the method was best when the standard deviation threshold from the mean of each selected class was set at 3. A total of 94,000 pixels were used as reference samples to train the parallelepiped classifier (approximately 35% of the total pixels) and the rest were used for testing.

Classification accuracy assessment

The accuracy of the classification results produced by PC method was evaluated by statistical measurements in a confusion matrix. The confusion matrix is a table that allows identification of confusion between the predicted classes and reference classes. Each row of the confusion matrix represents the pixels in a predicted class and each column represents the reference pixels in an actual class. The elements of the main diagonal of the confusion matrix represent the number of correctly classified pixels of each class while the elements above and below the main diagonal represent misclassified pixels.

Relevant statistical parameters, such as overall accuracy (OA), producer's (PA) and user's (UA) accuracies and kappa coefficient (κ), were computed from each confusion matrix associated with the individual case. The OA defined as the ratio of the total number of pixels correctly classified to the total number of pixels is calculated using Eq. (1):

$$\mathrm{OA} = \frac{\sum_{i=1}^{k} n_{ii}}{n}, \tag{1}$$

where k is the number of rows in the confusion matrix, n_{ii} is the number of pixels in row i and colon i of the confuzion matrix and n is the total number of pixels.

The UA and PA indicators provide information about commission errors (false positive) and omission errors (false negative) associated with the individual classes, respectively. The UA indicates the probability that a pixel predicted to be in a certain class really is that class. It is

defined by the ratio between diagonal value and total column value (user's accuracy = 100% − commission error). PA represents the probability that a value in a given class to be classified correctly. This indicator is defined by the ratio between diagonal value and total row value (producer's accuracy = 100% − omission error).

Kappa coefficient (κ) that corrects the OA of the classifier predictions by the accuracy expected to occur by chance [23] is defined by Eq. (2):

$$K = \frac{n\sum_{i=1}^{k} n_{ii} - \sum_{i=1}^{k} n_{i+}n_{+i}}{n^2 - \sum_{i=1}^{k} n_{i+}n_{+i}}, \quad (2)$$

where k, n_{ii} and n are as previously defined, n_{+i} is the total pixel number of row i and n_{+i} is the total pixel number of colon i.

The κ coefficient takes into account both the pixels on the main diagonal and the off-diagonal pixels of the confusion matrix (considering both in terms of classification results and reference pixels) to correct for random agreement between classes.

Results

Bone metastases detection using the PC-BS approach

We report here the results of the proposed parallelepiped classifier-based methodology for the detection of bone metastases in bone scintigraphy images (PC-BS) obtained on a lot of 12 patients with a mean age of 61.08 years (± 12.48) suspected with bone metastases.

The bone scintigraphy image and PC-BS classification results for a 60-year-old male patient suspected with bone metastases are shown in Fig. 2.

The PC-BS classification map (Fig. 2b) shows bone metastases (classes 6 and 7) located mainly in the mandible, shoulder, thoracolumbar spine and coxal bone. High radionuclide accumulation metastatic bone (class 6) covers 6192 pixels (2.41%), while very high radionuclide accumulation metastatic bone (class 7) covers only 535 pixels (0.21%) located in the spine, last rib, and lower part of the navel. Radionuclide accumulation levels for classes 6 and 7 are 110.21 ± 33.19 and 233.38 ± 28.53, respectively, showing high and very high levels of radionuclide accumulation. A number of 9241 pixels (3.6%) were identified as perimetastatic bone tissue with significant accumulation located mainly in the spine, sacral bone, and coxal bones. Normal bone tissue with variable radionuclide accumulation levels (classes 1–4) covers the rest of the skeleton.

Depending on the mean value of the pixel, we introduced an accumulation scale ranging from low (normal bone with low density) (level 1) to very high (level 7) for metastatic tissue with the highest accumulation level. The colour map produced by our classification method allows a better differentiation of the seven accumulation classes than the original gray level bone scintigraphy image. This is obvious an easier way to discern between classes due to better contrast.

Classification accuracy

A classification accuracy analysis was performed to quantitatively assess the performance of PC-BS method in terms of OA, PA, UA and kappa coefficient (κ) and to determine the quality of information provided by PC-BS classification results for bone metastasis detection. In this study, the accuracy of PC-BS method was estimated with the help of confusion matrix. Table 1 shows the confusion matrix for the PC-BS method for the particular case presented in Fig. 2.

The confusion matrix shown in Table 1 summarizes the classification results of 108,717 pixels. From this matrix, it can be seen that 93,910 pixels located along the main diagonal are correctly classified and 14,807 pixels located above and below the main diagonal are mistakenly classified. For example, the sixth column of the confusion matrix shows that 1511 (18.47%) pixels that should have been metastatic bone tissue with high radionuclide accumulation (class 6—red) were classified as perimetastatic bone tissue with significant radionuclide accumultion (class 5—orange) and 477 (5.83%) pixels were classified as metastatic bone tissue with very high accumulation level (class 7—maroon). On the other hand, the sixth line of the confusion matrix shows that 230 (2.27%) pixels were classified as perimetastatic bone tissue with significant accumulation (class 5—orange) although these pixels should have been metastatic bone tissue with high accumulation (class 6—red).

It can be noticed that there are only a few mutual misclassifications. The measure of such errors is the PA and, respectively, UA indicators calculated for each class. The value ranges of PA and UA indicators for the particular case presented above ranged from 71.03% (class 2) to 100% (classes 1 and 7), whereas the UA was found to be between 21.29% (class 7) and 96.42% (class 6) (Fig. 3).

The most commonly, mutual misclassifications are between perimetastatic bone tissue with significant accumulation and metastatic bone tissue with high accumulation as well as between metastatic bone tissue with high accumulation and metastatic bone tissue with very high accumulation which, from the point of view of bone metastases detection, is not a major impediment. Furthermore, classification results allow the identification of these types of bone tissue that cannot easily be distinguished visually from each other in the bone scintigraphy image.

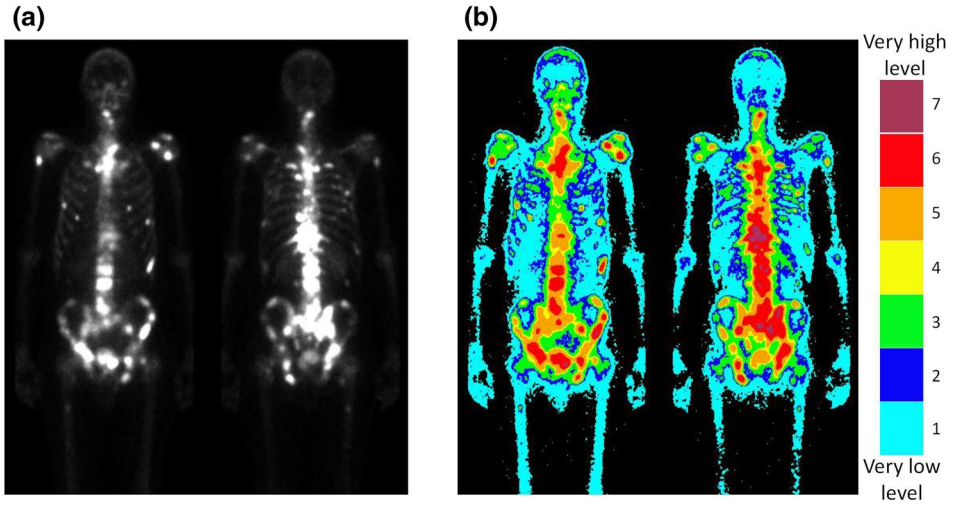

Fig. 2 The bone scintigraphy image and PC-BS classification map for a 60-year-old male patient suspected with bone metastases. **a** Anterior and posterior bone scintigraphy images; **b** PC-BS classification map; **c** size, pixel intensity and radionuclide accumulation level for different bone tissue type

(c)

Bone tissue type	Class Label	Class Color	Area (pixels)	Mean± SD (counts)	Radionuclid accumulation level
normal bone tissue with low density	1	cyan	49,463 (19.245%)	6.39±1.82	very low
normal bone tissue with intermediate low density	2	blue	16,614 (6.464%)	11.87±1.14	low
normal bone tissue with intermediate high density	3	green	16,903 (6.577%)	18.63±3.37	slightly below average
normal bone tissue with high density	4	yellow	4,861 (1.891%)	29.90±2.53	average
perimetastatic bone tissue with significant radionuclide accumulation	5	orange	9,241 (3.596%)	48.80±9.62	slightly above average
metastatic bone tissue with high radionuclide accumulation	6	red	6,192 (2.409%)	110.21±33.19	high
metastatic bone tissue with very high radionuclide accumulation	7	maroon	535 (0.208%)	233.38±28.53	very high

Table 1 Confusion matrix for PC-BS classification method

Class	Reference sample (pixels)								
	Class 1	Class 2	Class 3	Class 4	Class 5	Class 6	Class 7	Total	UA (%)
Classification results									
Class 1	40,147	6739	0	0	0	0	0	46,886	85.63
Class 2	0	16,521	3609	0	0	0	0	20,130	82.07
Class 3	0	0	16,903	783	0	0	0	17,686	95.57
Class 4	0	0	777	4777	681	0	0	6235	76,62
Class 5	0	0	0	0	9241	1511	0	10,752	85.95
Class 6	0	0	0	0	230	6192	0	6422	96.42
Class 7	0	0	0	0	0	477	129	606	21.29
Total	40,147	23,260	21,289	5560	10,152	8180	129	108,717	
PA (%)	100	71.03	79.4	85.92	91.03	75.7	100		
									OA = 86.38% κ = 0.8190

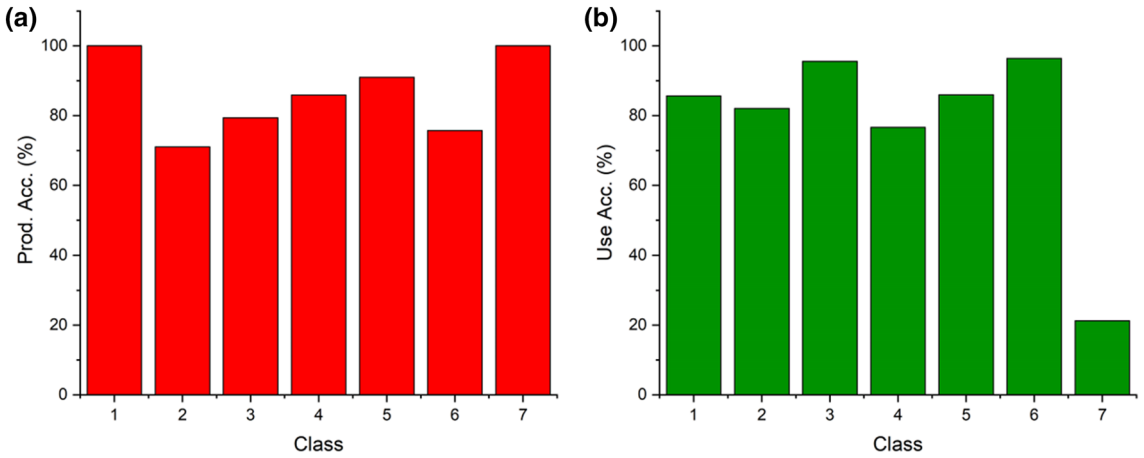

Fig. 3 The producer and user accuracies for different bone tissue types calculated for the 60-year-old male patient suspected with bone metastases. **a** Producer's accuracy; **b** user's accuracy

The overall classification accuracy (OA) for PC-BS method, calculated as the ratio between the total number of correctly classified pixels and the total number of pixels in the confusion matrix, was 86.38% for this particular case and the kappa coefficient (κ) was found to be above 0.8 ($\kappa = 0.8190$) indicating that there is an almost perfect agreement [24] between the classification results and the reference data.

For all bone scintigraphy images of the patients included in this study, PC-BS method performed well in terms of overall classification accuracy, PA, UA and κ coefficient (Fig. 4).

The average overall classification accuracy of the PC-BS method was found to be of $87.58 \pm 2.25\%$ and the average κ coefficient was 0.8367 ± 0.0252. The lowest producer accuracy found in the PC-BS classification was $71.06 \pm 1.33\%$ for normal bone tissue with intermediate low density (class 2) and the highest $98.15 \pm 2.21\%$ for metastatic bone tissue with very high radionuclide accumulation (class 7), whereas the UA ranged from $26.09 \pm 4.44\%$ (class 7) to $95.04 \pm 2.29\%$ (class 6—metastatic bone tissue with high radionuclide accumulation).

Metastatic bone tissue with very high radionuclide accumulation (class 7) has high values for producer accuracy in all cases, but low values for UA, meaning that some pixels from this class are omitted and the class underestimates in classification map. This might happen because of the small number of pixels belonging to this class. Moreover, some of these pixels were classified as being metastatic bone tissue with high radionuclide accumulation (class 6) (Table 1). Thus, a net differentiation between metastatic bone tissue with high radionuclide accumulation (class 6) and metastatic bone tissue with very high radionuclide accumulation (class 7) cannot be done, but this is not a major impediment for the bone metastases detection.

Therefore, the PC-BS method performed well enough in detecting bone metastases from bone scintigraphic images.

Discussion

Correct interpretation of the bone scintigraphy image is of paramount importance in choosing the treatment strategy, depending on the presence or absence of bone metastases. Visual examination of the bone scintigraphy bone image is a difficult pattern-recognition task even for physicians with long experience. Therefore, the need to develop objective methods for interpreting the scintigraphy image is a current research topic. Different computer-assisted diagnosis (CAD) systems for the interpretation of bone scintigraphy images have been investigated to date and two of them have recently become part of routine clinical work [16, 18].

In this work, we present a novel methodology for the detection of bone metastases in bone scintigraphy images based on the PC method. It uses the pixel values in a bone scintigraphy image to define individual bone classes with different radionuclide accumulation levels and generate bone classification maps. The method consists of a three-step sequence: bone scintigraphy image acquisition, bone scintigraphy image processing and PC method-based bone scintigraphy image analysis resulting in a bone classification map.

Recent studies report good results of artificial neural network (ANN)-based CAD systems for detection of bone metastasis [5, 16, 18]. However, an impairment of the performance of these ANN-CAD systems by training databases was also highlighted as possible.

The results presented here reveal that the proposed PC-BS method allows information extraction about seven types of bone tissue (normal and metastatic) that can be identified

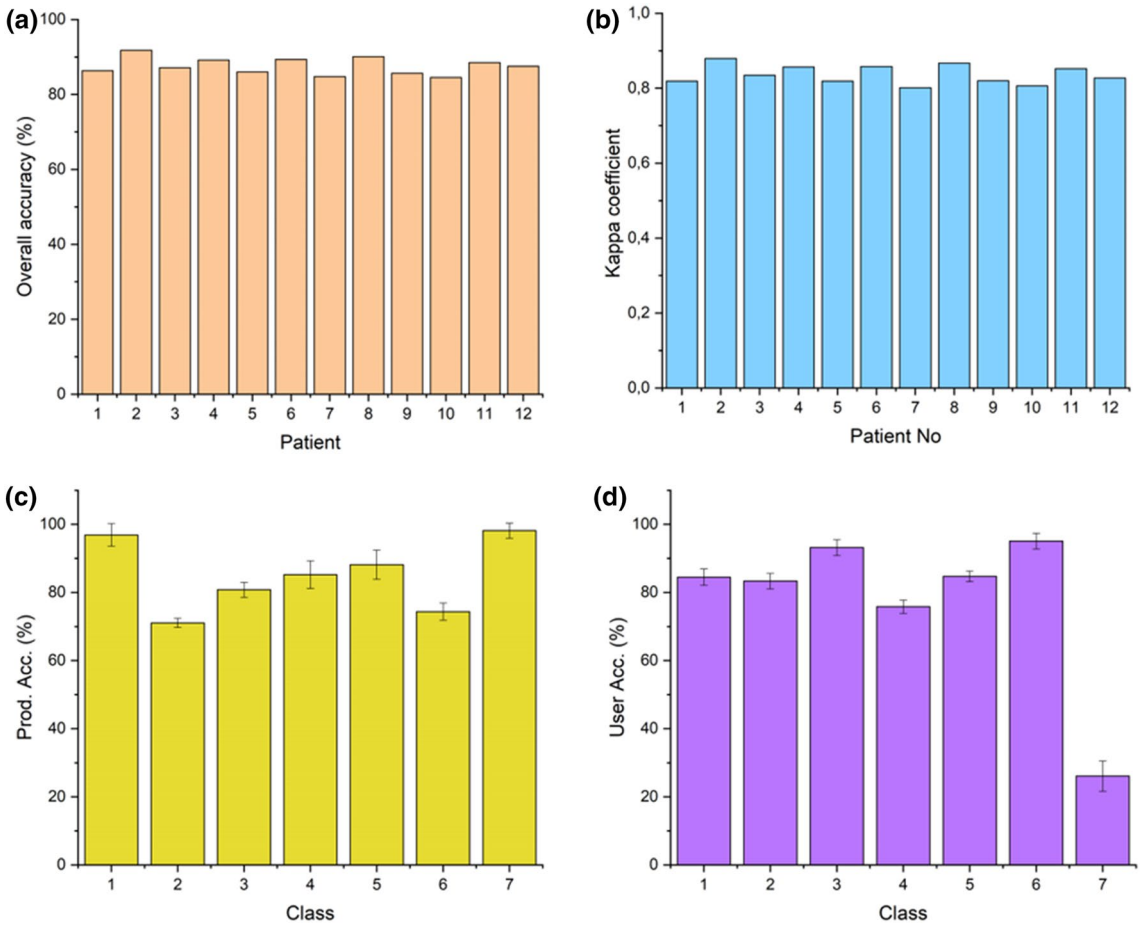

Fig. 4 Classification performance of the PC-BS method. **a** Overall accuracy; **b** κ coefficient; **c** producer's accuracy; **d** user's accuracy. Error bars represent one standard deviation from the mean

when bone scintigraphy data are used as input for the parallelepipedal classification method. Differentiating classes 6 and 7 from classes 1–4 is of paramount importance for an accurate diagnosis and taking the right decision. Class 5 is an intermediate bone tissue class and it is probably the threshold to diseased bone. The size, pixel intensity and radionuclide accumulation level for each bone tissue type can be calculated. The area size is taken into account when assessing the extent of bone lesions. Pixel intensity is a measure for differentiating tissue types and the radionuclide accumulation level indicates the presence of bone metastases (or inflammatory conditions) (e.g. Fig. 2b level 6 and 7). All these parameters can help physicians for a more accurate interpretation of the bone scintigraphy image.

Performances in bone metastases detection of PC-BS method proposed in the present study were assessed using confusion matrices. The results of PC-BS method were quite accurate in terms of OA and κ coefficient, despite abundant misclassifications found for different bone tissue types. The most misclassified bone tissue types were normal bone tissue with intermediate low density (class 2), normal bone tissue with intermediate high density (class 3) and normal bone tissue with high density (class 4). This happened probably because of similar accumulation characteristics of normal bone or difficulties in training the software due to the small dimensions of these regions on the skeleton with few pixels fitted to be fed. However, this is not important in terms of metastases identification. Classification errors were detected for class 5 which was classified as class 6, which cannot change the overall result as long as the border between normal and diseased bone is situated between classes 4 and 5. The classes were defined by an experienced radiologist and the existence of class 5 ("perimetastatic tissue") implies that tissue from class 6 should exist. That is why we decided that the threshold from normal to pathological should be between classes 4 and 5. As expected, classes 1 and 7 were best classified having the extreme levels of accumulation (the lowest and the highest). The classification map developed in the present study has the obvious advantage of better contrast compared to the original bone scintigraphy image. It can detect even small areas of diseased bone (depending on the dimensions of pixels), but some correlation with clinical

data has to be taken into account when metastatic tissue of small dimensions that cannot be detected on the original scintigraphy image becomes visible with our method.

The results presented here reveal that, by combining scintigraphy technique with parallelepipedal classification method, it is possible to accurately detect bone metastases. This new approach has proven to be accurate enough in bone metastases detection and may help physicians for a correct interpretation of bone scintigraphy image and a right treatment decision.

However, our study raises some interesting questions. It would be important to consider a validation step of PC-BS method results by comparison with other imaging technique such as X-rays, computed tomography, magnetic resonance imaging, positron emission tomography to confirm its performance. Furthermore, validation of the method on a larger group of patients is required. It is also important to improve the performance of the PC-BS method by identifying suitable methods for selecting reference samples (systematic or random methods) as well as establishing the optimal number of reference samples required to train the parallelepiped classifier. These questions will be addressed in the further studies.

Conclusions

In conclusion, the new parallelepiped classifier-based methodology for the detection of bone metastases presented in this study has proved to have the ability to facilitate an easier but correct interpretation of bone scintigraphy images, assisting the physician in detecting bone metastases, diagnostic process and making appropriate treatment decisions. These preliminary results are promising, but future research is needed to validate the method and improve the accuracy of scintigraphy image classification.

Author contributions All authors contributed to the study conception and design. Data acquisition was performed by F-GE. The data processing and analysis were performed by F-GE and MAC. Interpretation of the results was carried out by SVP and MAC. All authors contributed to the writing of the manuscript. All authors read and approved the final version of the manuscript.

Funding This study was funded by the Romanian Ministry of Research and Innovation (Grant number PN 33N/16.03.2018).

Compliance with ethical standards

Conflict of interest The authors declare that they have no conflict of interest.

Ethical approval All procedures performed in this study involving human participants were in accordance with the ethical standards of the "Saint John" Emergency Clinical Hospital Research Committee and with the 1964 Helsinki declaration and its later amendments or comparable ethical standards.

Informed consent Informed consent was obtained from all individual participants included in the study.

References

1. Coleman RE. (2001) Metastatic bone disease: clinical features, pathophysiology and treatment strategies. Cancer Treat Rev. 2001;27:165–76.
2. Lukaszewski B, Nazar J, Goch M, Lukaszewska M, Stepinski A, Jurczyk MU. Diagnostic methods for detection of bone metastases. Contemp Oncol (Pozn). 2017;21:98–103. https://doi.org/10.5114/wo.2017.68617.
3. Woolf DK, Padhani AR, Makris A. Assessing response to treatment of bone metastases from breast cancer: what should be the standard of care? Ann Oncol. 2015;26:1048–57. https://doi.org/10.1093/annonc/mdu558.
4. Del Vescovo R, Frauenfelder G, Francesco Giurazza F, et al. Role of whole-body diffusion-weighted MRI in detecting bone metastasis. Radiol Med (Torino). 2014;119:758–66. https://doi.org/10.1007/s11547-014-0395-y.
5. Nakajima K, Nakajima Y, Horikoshi H, et al. Enhanced diagnostic accuracy for quantitative bone scan using an artificial neural network system: a Japanese multi-center database project. EJNMMI Res. 2013;3:83. https://doi.org/10.1186/2191-219X-3-83.
6. Doi K. Computer-aided diagnosis in medical imaging: historical review, current status and future potential. Comput Med Imaging Graph. 2007;31:198–21111.
7. Taylor P, Potts HW. Computer aids and human second reading as interventions in screening mammography: two systematic reviews to compare effects on cancer detection and recall rate. Eur J Cancer. 2008;44:798–807.
8. Suzuki K. A supervised 'lesion-enhancement' filter by use of a massive-training artificial neural network (MTANN) in computer-aided diagnosis (CAD). Phys Med Biol. 2009;54:31–45.
9. Petrick N, Haider M, Summers RM, Yeshwant SC, Brown L, Iuliano EM, Louie A, Choi JR, Pickhardt PJ. CT colonography with computer-aided detection as a second reader: observer performance study. Radiology. 2008;246:148–56.
10. Mazzetti S, Giannini V, Russo F, Regge D. Computer-aided diagnosis of prostate cancer using multi-parametric MRI: comparison between PUN and Tofts models. Phys Med Biol. 2018;63:095004. https://doi.org/10.1088/1361-6560/aab956.
11. Kang KW, Chang HJ, Shim H, Kim YJ, Choi BW, Yang WI, Shim JY, Ha J, Chung N. Feasibility of an automatic computer-assisted algorithm for the detection of significant coronary artery disease in patients presenting with acute chest pain. Eur J Radiol. 2012;81:e640–e646646. https://doi.org/10.1016/j.ejrad.2012.01.017.
12. Dong ZC. Detection of subjects and brain regions related to Alzheimer's disease using 3D MRI scans based on eigenbrain and machine learning. Front Comput Neurosci. 2015;66:1–15.
13. Erdi YE, Humm JL, Imbriaco M, Yeung H, Larson SM. Quantitative bone metastases analysis based on image segmentation. J Nucl Med. 1997;38:1401–6.
14. Yin TK, Chiu NT. A computer-aided diagnosis for locating abnormalities in bone scintigraphy by a fuzzy system with a three-step minimization approach. IEEE Trans Med Imaging. 2004;23:639–54.

15. Sajn L, Kukar M, Kononenko I, Milcinski M. Computerized segmentation of whole-body bone scintigrams and its use in automated diagnostics. Comput Methods Progr Biomed. 2005;80:47–55.
16. Sadik M, Hamadeh I, Nordblom P, Suurkula M, Hoglund P, Ohlsson M, Edenbrandt L. Computer-assisted interpretation of planar whole-body bone scans. J Nucl Med. 2008;49:1958–65.
17. Kikuchi A, Onoguchi M, Horikoshi H, Sjostrand K, Edenbrandt L. Automated segmentation of the skeleton in whole-body bone scans: influence of difference in atlas. Nucl Med Commun. 2012;3:947–53.
18. Horikoshi H, Kikuchi A, Onoguchi M, Sjostrand K, Edenbrandt L. Computer-aided diagnosis system for bone scintigrams from Japanese patients: importance of training database. Ann Nucl Med. 2012;3:622–6.
19. Koizumi M, Miyaji N, Murata T, Motegi K, Miwa K, Koyama M, Terauchi T, Wagatsuma K, Kawakami K, Richter J. Evaluation of a revised version of computer-assisted diagnosis system, BONENAVI version 2.1.7, for bone scintigraphy in cancer patients. Ann Nucl Med. 2015;29:659–65.
20. Ogawa K, Sakata M, Li Y. Adaptive noise reduction of scintigrams with a wavelet transform. Int J Biomed Imaging. 2012. https://doi.org/10.1155/2012/130482 **(ID 130482)**.
21. Kuwahara M, Hachimura K, Ehiu S, Kinoshita M. Processing of riangiocardiographic images. Digit Process Biomed Images N Y. 1976;1980:187–203.
22. Schowengerdt RA. Remote sensing: models and methods for image processing. 3rd ed. San Diego: Academic Press; 1997. p. 411–412.
23. Cohen J. A coefficient of agreement for nominal scales. Educ Psychol Meas. 1960;20:37–46.
24. Landis JR, Koch GG. The measurement of observer agreement for categorical data. Biometrics. 1997;33:159–74.